

Optically Turbulent Femtosecond Light Guide in Air

M. Mlejnek, M. Kolesik, J. V. Moloney, and E. M. Wright

Arizona Center for Mathematical Sciences, and Optical Sciences Center, University of Arizona, Tucson, Arizona 85721
(Received 25 May 1999)

The onset and recurrence of multiple light filaments during the long-distance propagation of intense femtosecond infrared pulses in air is shown to share features with strong turbulence in other physical systems. Here, however, space-time collapse events drive the turbulence, and plasma defocusing, not dissipation, is the dominant mechanism regularizing the collapse.

PACS numbers: 42.65.Sf, 42.68.Ay

The nonlinear Schrödinger (NLS) equation in two or more dimensions is ubiquitous in physics, appearing as the canonical model for the description of wave collapse and strong turbulence phenomena. It appears as a universal model of weakly nonlinear, dispersive behavior in continuum mechanics, plasma physics, and optics, and examples include Langmuir waves in plasmas, mean field theory of weakly interacting Bose-Einstein condensates, and nonlinear pulse propagation in optical fibers. The reader is referred to the recent and excellent review by Robinson [1] in order to gain an appreciation for the broad scope of application of the NLS equation to strong turbulence phenomena. The picture that emerges in the strong turbulence scenario, irrespective of physical origin, is of a large collection of coexisting collapsing wave packets sustained by some background driving source and suffering dissipation at small spatial scales via a physical regularizing mechanism. The source of the collapse is the well-known self-similar blowup singularity of the higher-dimensional NLS equation which in two space dimensions carries exactly one critical power for self-focusing P_{cr} , whereas in three dimensions the collapse is termed supercritical and carries zero power.

The blowup singularity of the NLS description is clearly a mathematical artifact and some regularization mechanism must be invoked to prevent the extremely high intensities reached as the singularity is approached. Numerous suggestions have been made including higher-order perturbation corrections to the nonlinear wave equation, transit time damping in plasmas, and dissipation at the small spatial scales reached by the collapsing filament. For example, in Langmuir turbulence dissipation initiates when the characteristic spatial scale reaches the Debye length. The collapse singularity is also prevalent in nonlinear optics, causing critical self-focusing of laser beams and pulses in both gases and condensed media. Key regularization mechanisms include saturation of the nonlinear optical properties, nonlinear dissipation via multiphoton ionization (MPI), and avalanche ionization leading to optical breakdown and plasma absorption of the field.

In this Letter, we provide compelling numerical evidence that an optically turbulent, femtosecond light guide underlies the long-distance propagation of intense infrared

pulses in air, and there is now a considerable body of experimental evidence to support such a phenomenon [2–4]. In addition, in contrast to the usual strong turbulence scenario, here the turbulence is driven by collapsing light filaments in both space and time, and the dominant regularizing mechanism is nondissipative, namely, plasma defocusing. In particular, as the field collapses the intense light at the focus generates free electrons via MPI which in turn produce plasma defocusing which opposes the self-focusing, thereby regularizing the singularity with minimal loss of pulse energy. The present work is therefore an important step in understanding the nonlinear physics of long-distance pulse propagation in air and also expands the range of physical situations encompassed by the strong turbulence scenario.

Our basic physical model, which captures the essential features of long-distance propagation and is described in Ref. [5] along with parameter values appropriate to air, is a 3D + 1 dimensional NLS for the electric field envelope $\mathcal{E}(\mathbf{r}, t)$ coupled to a Drude model that describes the local plasma density $\rho(\mathbf{r}, t)$:

$$\begin{aligned} \frac{\partial \mathcal{E}}{\partial z} = & \frac{i}{2k} \nabla_{\perp}^2 \mathcal{E} - \frac{ik''}{2} \frac{\partial^2 \mathcal{E}}{\partial t^2} - \frac{\sigma}{2} (1 + i\omega\tau)\rho \mathcal{E} \\ & - \frac{\beta^{(K)}}{2} |\mathcal{E}|^{2K-2} \mathcal{E} + i \frac{\omega}{c} (1 - f)n_2 |\mathcal{E}|^2 \mathcal{E} \\ & + i \frac{\omega}{c} fn_2 \left[\int_{-\infty}^{\infty} dt' R(t - t') |\mathcal{E}(t')|^2 \right] \mathcal{E}, \quad (1) \end{aligned}$$

$$\frac{\partial \rho}{\partial t} = \frac{\sigma}{E_g} \rho |\mathcal{E}|^2 + \frac{\beta^{(K)} |\mathcal{E}|^{2K}}{K \hbar \omega}, \quad (2)$$

where drift and diffusion of the plasma are ignored on the femtosecond time scale of the pulses. Here the transverse Laplacian operator ∇_{\perp}^2 is two dimensional and describes transverse diffraction of the light field, and the remaining terms on the right-hand side represent group velocity dispersion (GVD), absorption and defocusing due to the electron plasma, MPI, and nonlinear self-focusing. In Eqs. (1) and (2) ω stands for the optical frequency, $|\mathcal{E}|^2$ is the intensity, $k = \omega/c$, $k'' = \partial^2 k / \partial \omega^2$, ρ is the electron density, σ is the cross section for inverse bremsstrahlung, τ is the electron collision time, $\beta^{(K)}$ is the K -photon

absorption coefficient, and the nonlinear change in refractive index for a continuous wave field is $n_2|\mathcal{E}|^2$. The normalized response function $R(t)$ accounts for delayed nonlinear effects due to rotational stimulated Raman scattering [6] with f the fraction of the delayed nonlinear optical response. The first term on the right-hand side of the density equation describes growth of the electron plasma by cascade ionization where E_g is the ionization potential, and the second term is the contribution of MPI. We note that in the density equation (2) we have neglected both the radiative and three-body recombination on the basis that they are not relevant on the femtosecond time scales of our simulations.

Previous simulations based on Eq. (1) restricted to cylindrical symmetry have shown that an intense femtosecond pulse forms an extended nonlinear self-focal region in which a narrow plasma filament is formed and underlies the observed long-distance propagation, at least for modest peak input powers [5]. This observation is consistent with the *moving focus model* [4] whereby different time slices of the pulse focus at different nonlinear focal lengths concomitant with the power in each slice. The *self-waveguiding model* [2] offers an alternative picture in which self-focusing and plasma defocusing combine to produce a self-guided filament. Beyond the initial stage of propagation, however, these models differ [2–4]. An alternative model of long-distance propagation distilled from numerical simulations is the *dynamic spatial replenishment model* [5]. Here the self-focused filament on the leading edge of the pulse generates a narrow region of plasma which strongly defocuses the remainder of the pulse. Once the intensity decreases at the back of the pulse, the plasma generation mechanism turns off and the pulse can again refocus. This sequence of events can repeat many times in principle. A very recent experiment supports this recurrent collapse mechanism [7].

The key issue we address here is how the above picture of long-distance propagation is impacted for input pulses with peak powers many times above critical when the cylindrical symmetry of the input beam may be broken via transverse modulational instability (MI) [8] leading to spatial beam breakup into collapsing filaments, the number of filaments being roughly proportional to one half of the number of critical powers. A recent experiment [9] used a terawatt peak power (\sim thousand critical powers), 110 fs laser pulse at 790 nm to propagate over a distance of about 12 km vertically into the atmosphere, and this highlights the importance of this issue. Basically, we find that for peak input powers a few times critical, P_{cr} being around 2 GW for air, the input beam initially breaks up into filaments via MI, but that they tend to merge into a central filament with increasing propagation which thereafter evolves according to the dynamic spatial replenishment model. An example of this is shown in Fig. 1 where we display the transverse distribution of the fluence, or time-integrated intensity,

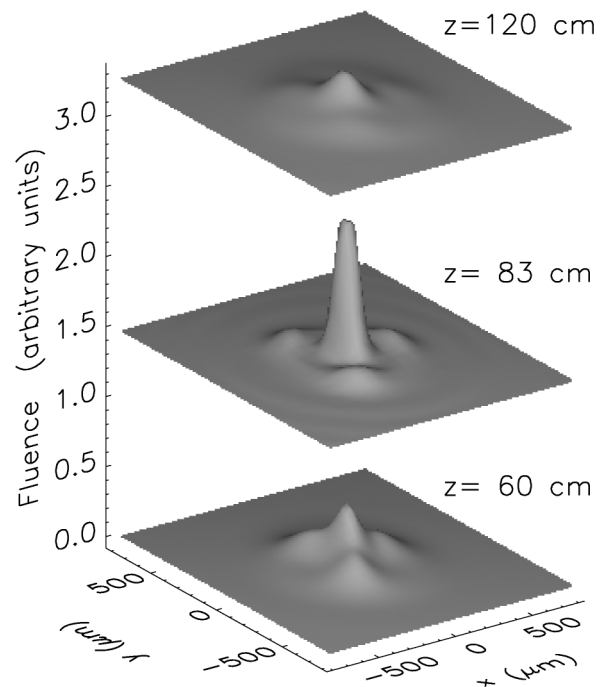


FIG. 1. Evolution of the total energy fluence at the distances $z = 0.60$ m, 0.83 m, 1.20 m in the case of perturbed super-Gaussian ($w_0 = 0.7$ mm) with $P = 4P_{cr}$. To avoid plotting multiple axes in this and the following figures we use arbitrary vertical offsets for the individual data sets.

for different propagation distances z and a peak input power $P = 4P_{cr}$, pulse duration 200 fs, and a perturbed super-Gaussian input beam of width 0.7 mm. Initially the input beam develops a transverse MI and three structures form around a central peak; see $z = 60$ cm. However, upon further propagation the central filament grows at the expense of the others, $z = 83$ cm, and thereafter dominates. In the later stages of propagation the central filament collapses and is absorbed and defocused by the generated plasma, and thereafter broadens spatially; see $z = 120$ cm.

In order to approach the issue of long-distance propagation for very high input powers, say $P > 20P_{cr}$, we need to simulate a situation where we have a sufficient density of collapsing light filaments with an accompanying background energy reservoir to regenerate recurrent collapses. This poses a formidable numerical challenge in order to resolve the spatial extent of the input beam and the collapsing filaments. To this end we have developed an adaptive (in time and in space) grid method which automatically uses multiple levels of fine-grid patches around collapse events while retaining a coarser grid to sample the background field. In addition we simulate the dynamics of the central portion of a broad Gaussian input beam of spot size w_0 by considering a square domain of side w_0 centered on the input with outgoing wave boundary conditions: This scheme greatly reduces the computational burden by concentrating the computational

effort on the high intensity region where filaments form. For the representative simulations presented here we chose a collimated, 200 fs Gaussian pulse centered at 775 nm with a beam waist of $w_0 = 0.7$ cm, and the peak power contained within our computational domain corresponds to $35P_{cr}$. Furthermore, to speed up the filament formation, and hence reduce the computational cost, we added a 15% field modulation at the spatial frequency of maximum growth rate for the transverse MI predicted on the basis of plane-wave theory using the peak intensity of the input beam [8]. For this strong initial perturbation the filament formation starts at about 8 m.

Representative results from our simulations are shown in Figs. 2–4: The perturbations added to the input Gaussian field first grow via MI and then begin to collapse between $z = 8$ –9 m. Figure 2 displays a sequence of movie frames showing the complex dynamics of the collapsing filaments for propagation distances $z = 9.0$, 9.9, 10.8, and 11.7 m. These isosurfaces of constant intensity are created by choosing threshold intensity at a level which arises only in a collapsing filament; thereby the filaments appear as “blobs” in the movie frames. Each picture corresponds to sweeping from the leading edge (left) to the trailing edge (right) of the pulse. By following the continuous evolution of the filaments between $z = 8$ –13 m in the form of movies we found that the filaments are created initially on the leading edge of the pulse and that they decay and recur on the trailing edge. However, the recurrence is not regular at fixed time intervals as in the radial symmetry case [5] as the filaments can merge before recurring as shown in Fig. 2 for $z = 9.9$ m. Figure 3 shows the transverse structure of the intensity filaments for three different time slices within the pulse at $z = 9.9$ m.

The top slice is near the leading edge of the pulse ($t \sim -100$ fs) and shows eight prominent spikes or collapsing filaments. The hollow regions surrounding each filament

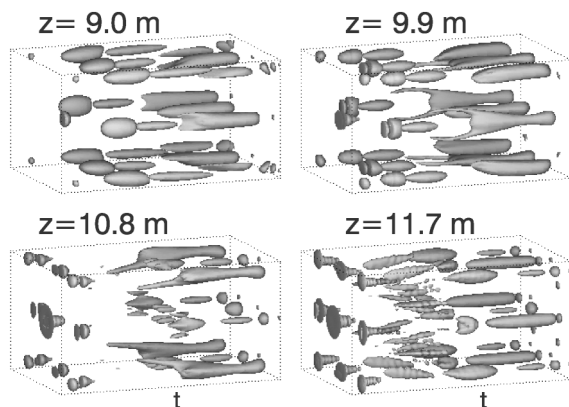


FIG. 2. Isosurfaces, showing details of the distribution of collapsing light filaments within a single pulse at propagation distances $z = 9.0, 9.9, 10.8, 11.7$ m. The initial power within the transversely truncated pulse $P = 35P_{cr}$.

represent light evacuated through the creation of a strong plasma induced defocusing lens, which regularizes the collapse: These light filaments then rapidly decay into the broad low intensity background. The light intensity within this low amplitude background reorganizes itself and a second recurrence of the collapse is observed around pulse center ($t \sim 40$ fs). This scenario repeats with a third recurrence near the back of the pulse ($t \sim 120$ fs). The complex spatial dynamics of the collapsing filaments is also evident in the fluence, often the experimentally accessible quantity, as is shown in Fig. 4 for different propagation distances. We note, however, that due to the turbulent nature of the field the filaments in the fluence become less pronounced with increasing propagation distance due to time averaging.

The above results highlight the main findings of our extensive numerical study of high-power long-distance propagation in air: The input beam initially breaks up due to transverse modulational instability in the leading edge of the pulse, and the collapsing filaments are subsequently regularized via plasma defocusing, and then are replenished and recur in the trailing portion of the pulse from the background energy reservoir. Furthermore, the filaments are also seen to merge and in this way they can maintain themselves with above critical peak power even though the field suffers some loss on each collapse cycle due to nonlinear absorption. Thus, for high input

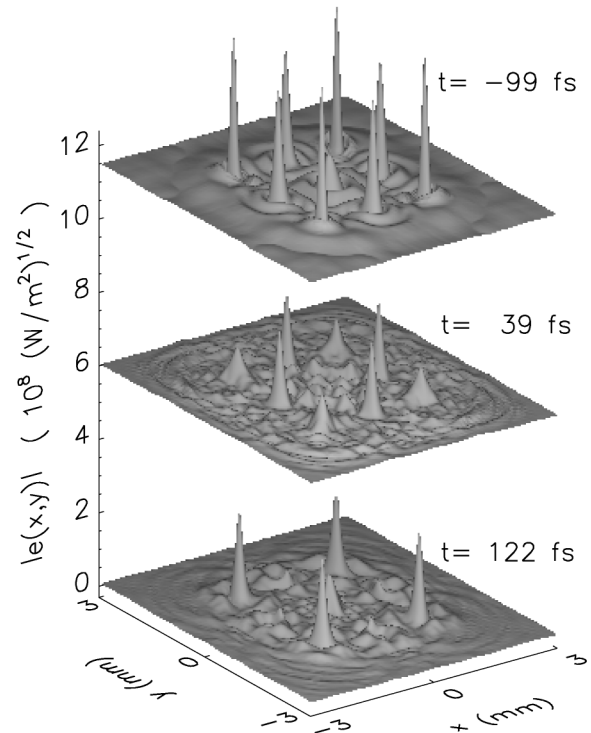


FIG. 3. Individual time slices within the pulse at propagation distance $z = 9.9$ m. The top frame shows the collapse near the leading edge of the pulse ($t = -99$ fs), the middle at the center ($t = 39$ fs), and the bottom near the trailing edge ($t = 122$ fs).

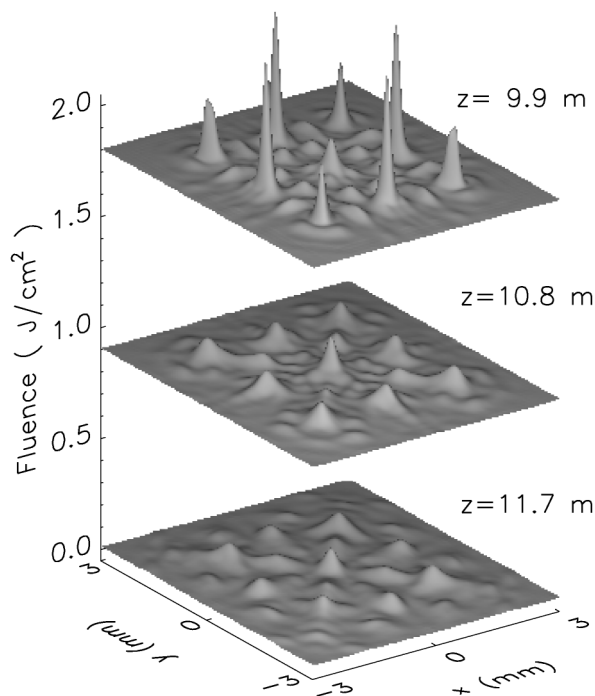


FIG. 4. Evolution of the total energy fluence at distances $z = 9.9, 10.8, 11.7$ m.

powers the notion of dynamic spatial replenishment as the mechanism of long-distance propagation still applies but now it is the strongly turbulent and recurrent collapse events fed by the background reservoir of energy which drive the process. We therefore term this phenomenon an optically turbulent light guide in contrast to the static self-waveguiding model proposed previously. However, in contrast to the usual strong turbulence scenario [1], here the collapse events are both in space and time, and the dominant regularizing mechanism is nondissipative, namely, plasma defocusing. In particular, from the simulations we estimate that a few percent of the input energy is lost during each collapse cycle indicating that plasma defocusing dominates over plasma absorption for the femtosecond pulses considered here. Physically, neglecting avalanche ionization effects for femtosecond pulses, the relative roles of plasma defocusing and plasma absorption are determined by the parameter $\omega\tau$ appearing in the third term on the right-hand side of Eq. (1), and in the air at 775 nm this product is $\omega\tau = 850$. ($\sigma\omega\tau/2 \approx 110 \text{ m}^{-1}$, $\omega n_2|\mathcal{E}|^2/c \approx 80 \text{ m}^{-1}$, $\beta^{(K)}|\mathcal{E}|^{2K-2/2} \approx 2 \text{ m}^{-1}$, for our parameters [5].) Furthermore, for $\lambda = 775$ nm, the GVD of air is positive (normal GVD) and this raises the additional possibility that normal GVD can arrest the collapse singularity by pulling the pulse apart along the time direction [10]. However, from the measured optical parameters of air, GVD does not become a significant player until well beyond the optical breakdown intensity ($I_{\text{th}} \approx 2 \times 10^{13} \text{ W cm}^{-2}$).

In conclusion, we have provided direct numerical evidence that a robust optically turbulent femtosecond light guide provides the physical basis for long-distance propagation in air. The sequence of events involves a modulational instability of a long wavelength low amplitude background which seeds the nucleation of a sea of critical collapsing filaments. The latter compress violently in both space and time until the peak intensity reaches the optical breakdown threshold for air, at which instant a strong plasma-induced defocusing lens is formed and the light is evacuated behind each filament. The amount of energy dissipation per filament is small, and most of the defocused optical energy is made available to the low amplitude background reservoir for further nucleation of filaments. The locations at which the intense optical filaments are generated are random in space and time. The scenario here reflects many of the features observed in strong turbulence. However, the primary arrest mechanism is not dissipation but refraction of light. In addition the interaction is driven by the low amplitude background within the pulse with no externally applied forcing and this persists over the input pulse duration. Despite the highly transient nature of the phenomenon, it is extremely robust and persists over long propagation distances.

We gratefully acknowledge discussions with N. Bloembergen, L. Berge, A. Talebpour, and V. Zakharov. Effort sponsored by the Air Force Office of Scientific Research, Air Force Materiel Command, USAF, under Grants No. AFOSR-97-1-0002 and No. AFOSR-98-1-0227.

-
- [1] P. A. Robinson, *Rev. Mod. Phys.* **62**, 507 (1997).
 - [2] A. Braun, G. Korn, X. Liu, D. Du, J. Squier, and G. Mourou, *Opt. Lett.* **20**, 73 (1995).
 - [3] E. T. J. Nibbering, P. F. Curley, G. Grillon, B. S. Prade, M. A. Franco, F. Salin, and A. Mysyrowicz, *Opt. Lett.* **21**, 62 (1996).
 - [4] A. Brodeur, C. Y. Chien, F. A. Ilkov, S. L. Chin, O. G. Kosareva, and V. P. Kandidov, *Opt. Lett.* **22**, 304 (1997).
 - [5] M. Mlejnek, E. M. Wright, and J. V. Moloney, *Opt. Lett.* **23**, 382 (1998).
 - [6] E. T. J. Nibbering, G. Grillon, M. A. Franco, B. S. Prade, and A. Mysyrowicz, *J. Opt. Soc. Am. B* **14**, 650 (1997).
 - [7] S. Petit, A. Talebpour, A. Proulx, and S. L. Chin, in *Proceedings of the 8th International Laser Physics Workshop, Budapest, Hungary, 1999* [*Laser Phys.* (to be published)].
 - [8] A. J. Campillo, S. L. Shapiro, and B. R. Suydam, *Appl. Phys. Lett.* **23**, 628 (1973).
 - [9] L. Wöste, C. Wedekind, H. Wille, P. Rairoux, B. Stein, S. Nikolov, C. Werner, S. Niedermeier, F. Ronneberger, H. Schillinger, and R. Sauerbrey, *Laser und Optoelektronik* **29**, 52 (1997).
 - [10] L. Berge, *Phys. Rep.* **303**, 259 (1998).